Two-stage Distributionally Robust Capacity Configuration Method for Shared Energy Storage Considering Flexibility and Uncertainty of Distributed Resources

Ning Zhang, *Student Member*, *IEEE*, Yanbo Chen, *Senior Member*, *IEEE*, Zhi Zhang, *Member*, *IEEE*, and Haoxin Tian, *Student Member*, *IEEE*

***Abstract*—Energy storage and generalized energy storage (GES) such as electric vehicles (EVs) and heating, ventilation, and air conditioning (HVAC) systems play a critical role in enhancing the flexibility of power systems. The shared system architecture can improve utilization rates of energy storage and reduce configuration costs. However, the heterogeneity and inherent uncertainty of GES pose significant challenges to the rational configuration and operation of energy storage. To address this, we employ a two-stage distributionally robust capacity configuration method for shared energy storage considering the flexibility and uncertainty of distributed resources. First, by integrating the operational characteristics of both physical and virtual energy storage, a shared system architecture is proposed for the GES. Second, to overcome the limitation of existing EV aggregation models, which are typically tailored for ideal battery behaviors, a more accurate aggregation model is introduced based on the parameter planning, termed the GES model. An uncertainty probability set modeling approach for demand-side resources is derived based on this model. Finally, considering the flexibility and uncertainty associated with EVs and HVAC systems, a distributionally robust optimization model for shared energy storage capacity configuration is proposed. Simulation results demonstrate that the proposed method increases the revenue of operators and the utilization of energy storage resources, while also reducing the configuration capacity.**

***Index Terms*—Generalized energy storage, demand-side resource, shared energy storage, capacity configuration, flexibility, uncertainty, distributionally robust optimization.**

Manuscript received: June 3, 2025; revised: September 5, 2025; accepted: October 22, 2025. Date of CrossCheck: October 22, 2025. Date of online publication: December 23, 2025.

This work was supported by the Smart Grid National Science and Technology Major Special Project (No. 2025ZD0807100).

N. Zhang, Y. Chen (corresponding author), Z. Zhang, and H. Tian are with the State Key Laboratory of Alternate Electrical Power System with Renewable Energy Sources and School of Electrical & Electronic Engineering, North China Electric Power University, Beijing 102206, China, and Y. Chen is also with the School of Engineering, Qinghai University of Science and Technology, Xining 810016, China, and School of Electrical Engineering, Jiangxi University of Water Resources and Electric Power, Nanchang 330099, China (e-mail: zhangn0328@163.com; yanbochen2008@sina.com.cn; zz_dqgc@163.com; 15932266891@163.com).

DOI: 10.35833/MPCE.2025.000508

I. Introduction

WITH the continued advancement of carbon peaking and carbon neutrality strategies, the demand side of the new-type power system is gradually shifting from traditional passive consumption to active production and consumption [1], [2]. The increasing scale of distributed resources on the demand side is posing greater challenges for the flexible regulation capability of power systems. In this context, energy storage has emerged as a key technology for enhancing the utilization of renewable energy and the flexibility of the demand side [3]. However, traditional physical energy storage (PES) devices are characterized by low utilization rates [4], high investment costs, and long payback periods [5], which constrain their widespread application. Given the large numbers, wide distributions, and flexible adjustabilities of demand-side resources such as electric vehicles (EVs) and heating, ventilation, and air conditioning (HVAC) systems, there is an urgent need to explore the energy storage potential of idle demand-side resources. Therefore, it is crucial to develop a more efficient and economical utilization system for generalized energy storage (GES) to achieve optimal energy storage configuration.

Shared energy storage (SES) enhances the utilization of energy storage resources while reducing the investment cost of energy storage by introducing a shared economy operating model based on traditional energy storage [6], [7]. In [8], an SES management system, a credit-based capacity and energy sharing pricing strategy, and an SES planning model are proposed. In [9], a dynamic optimal operation strategy for centralized SES station is proposed based on Nash bargaining theory. In [10], the energy storage planning problem is characterized as a distributionally robust optimization (DRO) model considering multiple uncertainties in wind power and photovoltaics. In [11], a collaborative capacity configuration model between a microgrid operator and an SES operator is proposed through a Nash bargaining game. In [12], a joint planning strategy for SES is proposed for large-scale prosumers, which utilizes multi-step clustering and generalized Nash bargaining. In [13], a real-time energy management strategy for SES is proposed to enhance the consumption of renewable energy and improve the stability of the power system supply. In [14], a model of an electricity-hydrogen SES configuration capable of supporting integrated energy systems is established, which enhances the economic viability of SES throughout its lifecycle.

Existing research on the SES configuration has focused primarily on PES. On the load side, distributed resources such as EVs and HVAC systems also have potential for energy storage use [15], which can be collectively referred to as GES. Centralized investment and unified regulation of diversified energy storage resources can achieve more aggregated and effective utilization of the energy storage industry chain. As a result, the investment and operation costs of energy storage services can be reduced, and the resource utilization efficiency can be improved. However, distributed resources are characterized by their large numbers, small capacities, diverse operating characteristics, and high uncertainties, making their aggregate behaviors difficult to model accurately. Many studies have explored GES models for temperature-controlled loads using methods such as Polyhedral method [16], supervised learning-assisted aggregation [17], virtual battery (VB) aggregation [18], [19], and optimization characterization [20]. In [21], VB models for EVs are proposed using an extreme energy scenario approach. In [22], a two-stage optimization framework that decouples scheduling and control strategies is introduced for aggregating distributed resources. In [23], a cluster aggregation model for EVs under ideal battery conditions is developed and jointly planned with HVAC clusters and PES. However, the current VB models for EVs fail to account for the charging and discharging efficiency of EVs. Furthermore, the variations in efficiency among EVs within a given cluster poses a challenge for accurately determining the aggregate efficiency. This, in turn, introduces potential inaccuracies in the external characteristics of the cluster and ambiguities in the definition of its controllable operating ranges.

The distributed resources such as EVs and HVAC systems are inherently uncertain [24]. Using deterministic models may therefore lead to failure in operational plans and unreliable optimization results [25]. In contrast, the GES model leverages the complementary nature of the units within a cluster. It mitigates the randomness of individual devices before aggregation, thereby enhancing the reliability of planning and scheduling. A key challenge is how to account for the uncertainty of GES in planning models. Existing literature typically uses stochastic optimization (SO) [26] and robust optimization (RO) [27] to address uncertainty. However, these methods tend to be either overly conservative or overly aggressive in modeling flexible supply and demand. In [23], the uncertainty problem is approximated as a discrete chance-constrained problem based on value at risk. DRO model combines the advantages of both SO and RO [28], balancing conservatism with economic considerations, making it an effective approach for optimizing uncertainty in distributed resources. Resources such as EVs and HVAC systems, which are highly stochastic due to user behavior, cannot be accurately modeled using deterministic approaches. This leads to inaccurate aggregation and inefficient configuration. However, few studies have examined how uncertainties of demand-side resources affect the aggregation of GES and the configuration of SES.

The existing configurations of SES on the demand side exhibit the following shortcomings.

1) The energy storage characteristics of demand-side resources have not yet been incorporated into the planning and operational framework of SES.

2) Accurate aggregation model for demand-side resources is urgently needed to precisely characterize their flexible operating region and external characteristics.

3) The failure to account for uncertainties of demand-side resources is a critical shortcoming in existing capacity configuration methods for SES.

This study proposes a two-stage distributionally robust capacity configuration method that considers flexibility and the uncertainty of distributed resources. The main contributions of this paper are as follows.

1) The shared system architecture, including PES and virtual energy storage, is developed to enable their participation in the operation of SES. The proposed architecture integrates distributed resources for aggregation, storage, and sharing, fully exploiting their inherent energy storage potential and thereby enhancing the utilization efficiency of existing storage assets.

2) To address the challenges in quantifying the charging and discharging efficiency of EV clusters, a GES model for EV clusters is proposed for the aggregate representation of their external characteristics. Building on this, an uncertainty probability set modeling approach is established for EV and HVAC clusters, enabling an effective quantification of the uncertain characteristics of these clusters.

3) Considering the uncertainty of demand-side resources, a DRO model for shared energy storage capacity configuration is proposed using the uncertainty probability set modeling approach. This approach enables the derivation of an optimal investment strategy for SES that balances economic efficiency with operational robustness.

The rest of this paper is organized as follows. In Section II, a shared system architecture for the GES is presented. Section III presents the GES models and uncertainty probability set modeling approach for distributed resources. Section IV presents the two-stage distributionally robust capacity configuration method for SES considering the flexibility and uncertainty of distributed resources. Section V gives the DRO model solving algorithm. Section VI presents the simulation results. Finally, Section VII gives the conclusions.

II. Shared System Architecture for GES

In traditional SES application scenarios, SES operators configure and operate PES devices to meet the energy storage demands of multiple users within a region. Building upon the traditional SES framework, a shared system architecture for GES is proposed, as shown in Fig. 1. This architecture enables the aggregation and sharing of distributed energy storage resources through the integration of PES technologies, virtual energy storage technologies, and the shared economy concept. By establishing a generalized SES station, it effectively matches diverse energy storage suppliers with users, thereby optimizing resource allocation.

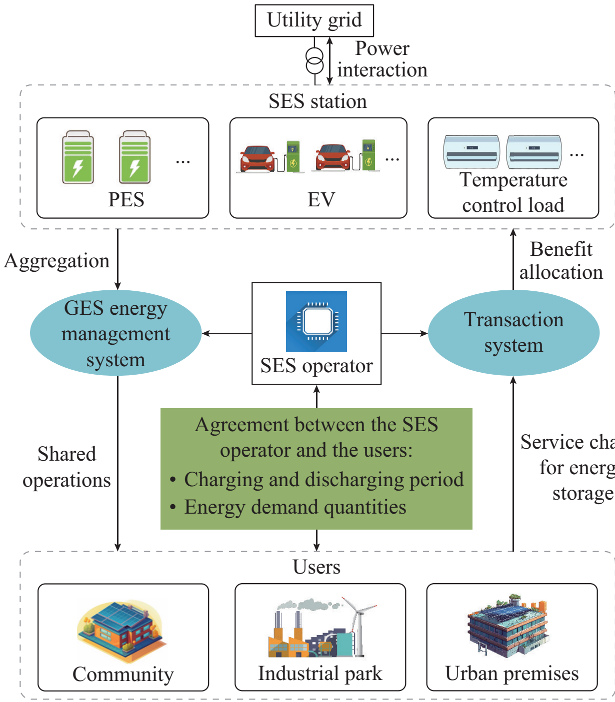

Fig. 1. Shared system architecture for GES.

GES has flexible power dispatch capabilities, enabling it to partially take over the role of SES and reduce capacity configuration costs. In the planning phase, SES operators determine the configuration capacity of PES based on user demand and the dispatchable potential of GES across scenarios. In the scheduling phase, operators create charging and discharging schedules of various energy storage devices according to their specific characteristics. Appropriate economic compensation is provided to the owners of the participating EVs and HVAC systems. If an SES station fails to deliver the contracted charging or discharging power, it must purchase the power shortfall from the grid.

The SES operator allows distributed resource holders on the demand side to participate in the scheduling of SES stations, leasing their idle energy storage capacity to those in need and earning corresponding profits. The SES operator signs service agreements with each user to provide charging and discharging services of SES. Users sign these service agreements based on their load forecast results. The service agreements include energy storage charging and discharging periods and energy demand quantities. The operation model of an SES station typically uses a fixed-rate tariff for users. Then, by leveraging the energy storage characteristics of the SES station, the operation model maximizes profits through arbitrage.

III. GES Models and Uncertainty Probability Set Modeling Approach for Distributed Resources

To exploit the regulation potential of demand-side resources, aggregation modeling is essential. The aggregation models obtained through the parameter planning are termed the GES model. This model offers a quantitative approach for assessing the flexibility of diverse resources such as EVs, HVAC systems, and PES devices by utilizing standardized energy storage parameters. Different resources exhibit distinct clustering characteristics. For example, the GES parameters of EV clusters and HVAC clusters are related to their operating states. Based on the established GES model, an uncertainty probability set modeling approach is proposed for addressing the uncertainties associated with EV and HVAC clusters, which quantifies the uncertain characteristics of demand-side resource clusters.

As the GES model for HVAC clusters has been well established in [20], this paper focuses on deriving the GES model for EV clusters.

A. GES Model for EV Clusters

In this subsection, a GES model considering EV charging and discharging efficiencies is derived to obtain accurate external characterization and aggregation control ranges for EV clusters.

1) Modeling of GES Model for Individual EV

First, the SES operator integrates key information for each EV, including the estimated arrival time, estimated departure time, and state of charge (SOC) upon connecting to the microgrid. On this basis, the ideal battery operation boundary for a single EV, as proposed in [21], is extended to a GES model for individual EV that accounts for charging and discharging efficiencies, thereby defining the flexible operation region for both capacity and power.

$$\bar{X}^{\mathrm{r}}_{i,t}=\min\{X^{\mathrm{a}}_i+\eta^{\mathrm{cha}}_i P^{\max}_i (t-T^{\mathrm{a}}_i)\tau, X^{\max}_i\}\quad t\in(T^{\mathrm{a}}_i,T^{\mathrm{d}}_i) \tag{1}$$

$$\underline{X}^{(1)}_{i,t}=\max\{X^{\mathrm{a}}_i+P^{\min}_i(t-T^{\mathrm{a}}_i)\tau/\eta^{\mathrm{dis}}_i, X^{\min}_i\}\quad t\in(T^{\mathrm{a}}_i,T^{\mathrm{d}}_i) \tag{2}$$

$$\underline{X}^{(2)}_{i,t}=\max\{X^{\mathrm{ex}}_i-\eta^{\mathrm{cha}}_i P^{\max}_i(T^{\mathrm{d}}_i-t)\tau, X^{\min}_i\}\quad t\in(T^{\mathrm{a}}_i,T^{\mathrm{d}}_i) \tag{3}$$

$$\underline{X}^{\mathrm{r}}_{i,t}=\max\{\underline{X}^{(1)}_{i,t},\underline{X}^{(2)}_{i,t}\}\quad t\in(T^{\mathrm{a}}_i,T^{\mathrm{d}}_i) \tag{4}$$

$$\bar{P}^{\mathrm{EV}}_{i,t}=\min\{(\bar{X}^{\mathrm{EV}}_{i,t+1}-\underline{X}^{\mathrm{r}}_{i,t})/(\eta^{\mathrm{cha}}_i\tau), P^{\max}_i\}\quad t\in(T^{\mathrm{a}}_i,T^{\mathrm{d}}_i-1) \tag{5}$$

$$\underline{P}^{\mathrm{EV}}_{i,t}=\max\{\eta^{\mathrm{dis}}_i(\underline{X}^{\mathrm{EV}}_{i,t+1}-\bar{X}^{\mathrm{r}}_{i,t})/\tau, P^{\min}_i\}\quad t\in(T^{\mathrm{a}}_i,T^{\mathrm{d}}_i-1) \tag{6}$$

where t is the time period index; $\bar{X}^{\mathrm{r}}_{i,t}$ and $\underline{X}^{\mathrm{r}}_{i,t}$ are the upper and lower limits of the feasible region of actual capacity of EV i, respectively; X^{a}_i is the initial capacity of EV i when it is connected to the grid; $P^{\min}_i$ and $P^{\max}_i$ are the lower and upper limits of charging and discharging power of EV i, respectively; $X^{\min}_i$ and $X^{\max}_i$ are the lower and upper limits of capacity of EV i, respectively; τ is the time step; $\underline{X}^{(1)}_{i,t}$ is the lower limit of capacity of EV i that is limited by both the discharging power and the minimum battery capacity; $\underline{X}^{(2)}_{i,t}$ is the lower limit of capacity of EV i that is limited by both the expected EV capacity and the minimum battery capacity; X^{ex}_i is the expected capacity of EV i that is needed at the departure time; T^{a}_i and T^{d}_i are the grid-connected time and off-grid time of EV i, respectively; η^{cha}_i and η^{dis}_i are the charging and discharging efficiencies of EV i, respectively; and $\bar{P}^{\mathrm{EV}}_{i,t}$ and $\underline{P}^{\mathrm{EV}}_{i,t}$ are the upper and lower limits of the flexible operation region of GES power of EV i, respectively. This yields the flexible operation region of individual EV.

2) Modeling of GES Model for EV Clusters

Accurately quantifying the overall charging and discharging efficiencies of a cluster is challenging, due to the large number of EVs and the wide variation in their individual charging and discharging efficiencies. Therefore, the GES model is used. Figure 2 illustrates the principle of the GES model for EV clusters, where X_{actual} is the feasible region of actual capacity; X_{ideal} is the feasible region of ideal capacity; and X_{ideal} is the feasible region of cluster capacity. The boundary parameter of the actual capacity is mapped to that of the ideal capacity, and the external characteristics of EV clusters are modeled as ideal batteries. Consequently, an aggregation model for EV cluster incorporating individual charging and discharging efficiencies is developed.

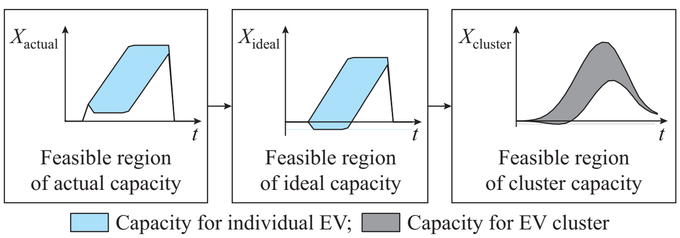

Fig. 2. Principle of GES model for EV clusters.

The optimization problems, with (7) and (8) as objective functions and (9) as constraints, are first solved to obtain the operating power when all EVs are maintained at their upper and lower capacity limits. The external power values $P_{i,t}$ obtained from the two optimization problems are denoted as $P_{i,t}^{\text{r},+}$ and $P_{i,t}^{\text{r},-}$, respectively.

$$\min \sum_{t=1}^{T}\sum_{i=1}^{N_{\text{ev}}}(X_{i,t}-\bar{X}_{i,t}^{\text{r}})^2 \tag{7}$$

$$\min \sum_{t=1}^{T}\sum_{i=1}^{N_{\text{ev}}}(X_{i,t}-\underline{X}_{i,t}^{\text{r}})^2 \tag{8}$$

s.t.

$$\begin{cases} X_{i,t+1}=X_{i,t}+\eta_i^{\text{cha}}P_{i,t}^{\text{cha}}+P_{i,t}^{\text{dis}}/\eta_i^{\text{dis}} \\ \underline{X}_{i,t}^{\text{r}}\leq X_{i,t}\leq \bar{X}_{i,t}^{\text{r}} \\ P_{i,t}=P_{i,t}^{\text{cha}}-P_{i,t}^{\text{dis}} \\ 0\leq P_{i,t}^{\text{cha}}\leq u_{i,t}^{\text{cha}}\bar{P}_{i,t}^{\text{EV}} \\ 0\leq P_{i,t}^{\text{dis}}\leq -u_{i,t}^{\text{dis}}\underline{P}_{i,t}^{\text{EV}} \\ u_{i,t}^{\text{cha}}+u_{i,t}^{\text{dis}}\leq 1 \\ T_i^{\text{a}}\leq t\leq T_i^{\text{d}}-1 \end{cases} \tag{9}$$

where $X_{i,t}$ is the capacity of EV i; T is the dispatch cycle; N_{ev} is the number of EVs in the cluster; $P_{i,t}^{\text{cha}}$ and $P_{i,t}^{\text{dis}}$ are the charging and discharging power of EV i, respectively; and $u_{i,t}^{\text{cha}}$ and $u_{i,t}^{\text{dis}}$ are the charging and discharging state variables of EV i, respectively, with $u_{i,t}^{\text{cha}}=1$ indicating charging and $u_{i,t}^{\text{dis}}=1$ indicating discharging.

Consequently, according to parameter planning, the feasible power region of the EV cluster, bounded by the upper limit $\bar{P}_t^{\text{EV}}$ and the lower limit $\underline{P}_t^{\text{EV}}$, is defined by summing the dispatchable power of all EVs, as shown in (10) and (11). The actual dispatchable capacity of EVs is converted to the ideal power. The upper and lower limits $\bar{X}_t^{\text{EV}}$ and $\underline{X}_t^{\text{EV}}$ of the feasible operation region of GES capacity are then given by the sum of the respective limits across the EV clusters, as expressed in (12) and (13), respectively.

$$\bar{P}_t^{\text{EV}}=\sum_{i=1}^{N_{\text{ev}}}\bar{P}_{i,t}^{\text{EV}}u_{i,t} \tag{10}$$

$$\underline{P}_t^{\text{EV}}=\sum_{i=1}^{N_{\text{ev}}}\underline{P}_{i,t}^{\text{EV}}u_{i,t} \tag{11}$$

$$\bar{X}_t^{\text{EV}}=\sum_{z=1}^{t}\sum_{i=1}^{N_{\text{ev}}}P_{i,z}^{\text{r},+}\tau \tag{12}$$

$$\underline{X}_t^{\text{EV}}=\sum_{z=1}^{t}\sum_{i=1}^{N_{\text{ev}}}P_{i,z}^{\text{r},-}\tau \tag{13}$$

where $z\in\{1,2,\ldots,t\}$ is the time index; and $u_{i,t}$ is the grid-connected state of EV i (1 for grid-connected, 0 for the off-grid).

Once an EV leaves the grid, it can no longer participate in the GES schedule and must therefore deduct this portion of its capacity, which can be characterized as:

$$X_t^{\text{exchange}}=\sum_{i=1}^{N_{\text{ev}}}X_i^{\text{ex}}(u_{i,t}-u_{i,t-1}) \tag{14}$$

where X_t^{exchange} is the off-grid capacity of the EV cluster during time period t.

By integrating the above models, the flexible operation region of GES capacity and power for EV clusters is derived as follows:

$$\underline{X}_t^{\text{EV}}\leq X_t^{\text{EV}}\leq \bar{X}_t^{\text{EV}} \tag{15}$$

$$\underline{P}_t^{\text{EV}}\leq P_t^{\text{EV}}\leq \bar{P}_t^{\text{EV}} \tag{16}$$

$$X_{t+1}^{\text{EV}}=X_t^{\text{EV}}+P_t^{\text{EV}}\tau+X_{t+1}^{\text{exchange}} \tag{17}$$

where X_t^{EV} and P_t^{EV} are the GES capacity and power of the EV cluster, respectively, with positive and negative values corresponding to the charging and discharging of GES.

The model (15)-(17) faithfully represents the external characteristics and aggregation regulation range of EV clusters, while considering the charging and discharging efficiency of individual EV.

B. GES Model for HVAC Clusters

The GES model for HVAC clusters can be constructed analogously to that for EV clusters. The parameter planning method maps the boundary parameters of temperature to those of capacity of an ideal battery, thereby establishing the external representation and defining the aggregation regulation range for HVAC clusters, as expressed in (18)-(20).

$$\underline{X}_t^{\text{HVAC}}\leq X_t^{\text{HVAC}}\leq \bar{X}_t^{\text{HVAC}} \tag{18}$$

$$\underline{P}_t^{\text{HVAC}}\leq P_t^{\text{HVAC}}\leq \bar{P}_t^{\text{HVAC}} \tag{19}$$

$$X_{t+1}^{\text{HVAC}}=\alpha^{\text{HVAC}}X_t^{\text{HVAC}}+P_t^{\text{HVAC}}\tau \tag{20}$$

where X_t^{HVAC} and P_t^{HVAC} are the GES capacity and power of the HVAC cluster, respectively; $\bar{X}_t^{\text{HVAC}}$ and $\underline{X}_t^{\text{HVAC}}$ are the upper and lower limits of GES capacity of the HVAC cluster, respectively; $\bar{P}_t^{\text{HVAC}}$ and $\underline{P}_t^{\text{HVAC}}$ are the upper and lower power limits of GES power of the HVAC cluster, respectively;

and α^{HVAC} is the mean value of the dissipation coefficient of the GES cluster. The detailed derivation process can be found in [20].

C. Uncertainty Probability Set Modeling Approach for EV and HVAC Clusters

Since the flexible operation regions for the GES capacity of EV and HVAC clusters are susceptible to stochastic user behavior, planning and operation based on the aforementioned deterministic model carry a risk of failure. Furthermore, the uncertainty probability sets for EV and HVAC clusters are difficult to obtain. Thus, this paper employs a data-driven approach to construct M stochastic scenarios for EV clusters and HVAC clusters from historical datasets. The ambiguous variable set for the individual EV in each scenario ξ^{ev} includes the grid connection time, disconnection time, initial SOC, and expected SOC. The ambiguous variable set for the individual HVAC system in each scenario ξ^{hvac} includes set temperature $\theta_{i,\mathrm{set}}$, thermal capacitance C_i, and thermal resistance R_i.

$$\begin{cases} \xi^{\mathrm{ev}} = \{T_i^{\mathrm{a}}, T_i^{\mathrm{d}}, X_i^{\mathrm{a}}, X_i^{\mathrm{ex}}\} \\ \xi^{\mathrm{hvac}} = \{\theta_{i,\mathrm{set}}, C_i, R_i\} \end{cases} \tag{21}$$

The proposed GES models for EV and HVAC clusters employed to construct their respective ambiguous variable sets ξ^{EV} for the EV clusters and ξ^{HVAC} for the HVAC clusters. These sets are derived from the aforementioned base variables, as expressed by:

$$\begin{cases} \xi^{\mathrm{EV}} = \{\underline{X}_t^{\mathrm{EV}}, \bar{X}_t^{\mathrm{EV}}, \underline{P}_t^{\mathrm{EV}}, \bar{P}_t^{\mathrm{EV}}, X_t^{\mathrm{exchange}}\} \\ \xi^{\mathrm{HVAC}} = \{\underline{X}_t^{\mathrm{HVAC}}, \bar{X}_t^{\mathrm{HVAC}}, \underline{P}_t^{\mathrm{HVAC}}, \bar{P}_t^{\mathrm{HVAC}}, P_{\mathrm{base},t}^{\mathrm{HVAC}}\} \end{cases} \tag{22}$$

where $P_{\mathrm{base},t}^{\mathrm{HVAC}}$ is the baseline power of the HVAC cluster, and its calculation method is referenced from [20].

Computations are performed separately on M samples of historical data from both the EV and HVAC clusters using the GES ambiguous variable sets. This is followed by the application of the K-means clustering algorithm, thereby deriving J discrete typical scenarios with their initial probability distribution. Given that each scenario retains inherent uncertainty, a comprehensive norm constraint is constructed around this initial distribution. This constraint, which includes the 1-norm and ∞-norm, confines the probability distribution of the uncertain scenarios within a reasonable fluctuation range, which can be expressed as:

$$\left\| p_j - p_j^0 \right\|_1 = \sum_{j=1}^{J} \left| p_j - p_j^0 \right| \le \rho_1 \tag{23}$$

$$\left\| p_j - p_j^0 \right\|_\infty = \max_{1 \le j \le J} \left| p_j - p_j^0 \right| \le \rho_\infty \tag{24}$$

where p_j^0 is the initial probability distribution value of scenario j; p_j is the probability distribution value of scenario j; and ρ_1 and ρ_∞ are the permissible ranges of probability distributions under the constraints of the 1-norm and ∞-norm, respectively. Larger values of ρ_1 and ρ_∞ imply a wider range of admissible distributions and thus stronger robustness. The probability distribution must satisfy the following confidence constraints:

$$\Pr\left\{ \sum_{j=1}^{J} \left| p_j - p_j^0 \right| \le \rho_1 \right\} \ge 1 - 2J\mathrm{e}^{-\frac{2M\rho_1}{J}} = \alpha_1 \tag{25}$$

$$\Pr\left\{ \max_{1 \le j \le J} \left| p_j - p_j^0 \right| \le \rho_\infty \right\} \ge 1 - 2J\mathrm{e}^{-2M\rho_\infty} = \alpha_\infty \tag{26}$$

where α_1 and α_∞ are the uncertainty probability confidence levels, from which the equations for the calculation of ρ_1 and ρ_∞ are obtained as:

$$\rho_1 = \frac{J}{2M} \ln \frac{2J}{1 - \alpha_1} \tag{27}$$

$$\rho_\infty = \frac{1}{2M} \ln \frac{2J}{1 - \alpha_\infty} \tag{28}$$

The ambiguous variable set Ω for the flexible operation region of GES capacity is formulated based on the comprehensive norm constraint. It can be observed that as the number of sample sizes approaches infinity, the reference distribution converges to the true distribution under the constraints of the 1-norm and ∞-norm.

$$\Omega = \left\{ \boldsymbol{p} = (p_j), j = 1, 2, \ldots, J | 0 \le p_j \le 1, \sum_{j=1}^{J} p_j = 1, \right. \\ \left. \sum_{j=1}^{J} \left| p_j - p_j^0 \right| \le \rho_1, \max_{1 \le j \le J} \left| p_j - p_j^0 \right| \le \rho_\infty \right\} \tag{29}$$

where $\boldsymbol{p}$ is the scenario probability distribution vector of the EV and HVAC clusters.

IV. Two-stage Distributionally Robust Capacity Configuration Method

By leveraging the proposed GES models for EV and HVAC clusters, these clusters can participate as GES in the capacity configuration and operation of SES station, aiming to reduce the PES investment costs and improve utilization efficiency.

A. Objective Function

Driven by the energy storage requirements of users, the SES operator aims to minimize the average daily total cost over the planning period. This total cost comprises two components: the equivalent daily investment cost F_{in} and the typical scenario operation cost F_{op}. The DRO model proposed in this study is a two-stage model with a three-layer "min-max-min" structure. In the first stage, the objective is to minimize the SES configuration cost, with the configuration capacity serving as the decision variable. The second stage aims to minimize the scheduling cost under the worst-case probability distribution of scenarios. The objective function is as follows:

$$F_{\mathrm{total}} = \min \left(F_{\mathrm{in}} + \max_{p_j \in \Omega} \sum_{j=1}^{J} p_j \min F_{\mathrm{op}} \right) \tag{30}$$

$$F_{\mathrm{op}} = C_{\mathrm{ma}}^{\mathrm{ES}} + C_{\mathrm{de}} + C_{\mathrm{EV}} + C_{\mathrm{HVAC}} - R_{\mathrm{grid}} - R_{\mathrm{sv}} - R_{\mathrm{tr}} \tag{31}$$

where $C_{\mathrm{ma}}^{\mathrm{ES}}$ is the cost of maintaining the PES; C_{de} is the loss cost of PES; C_{EV} is the scheduling compensation cost of EV clusters; C_{HVAC} is the scheduling compensation cost of

HVAC clusters; R_{grid} is the net revenue from grid electricity trading, calculated as the income from sales minus the cost of purchases made to fulfill user agreements; R_{sv} is the revenue generated from providing energy storage services (charging and discharging) to users; and R_{tr} is the revenue gained from trading electricity between the SES station and the user (the SES station pays the user a certain compensation when the user is charging and charges the user a certain fee when the user is discharging).

The specific expressions for each cost and revenue are given as:

$$F_{\text{in}}=\frac{1}{365}\frac{r(1+r)^{Y}}{(1+r)^{Y}-1}(c_{\text{in}}^{\text{X}}\bar{X}_{\text{in}}^{\text{ES}}+c_{\text{in}}^{\text{P}}\bar{P}_{\text{in}}^{\text{ES}})\tau \tag{32}$$

$$C_{\text{ma}}^{\text{ES}}=c_{\text{ma}}\bar{P}_{\text{in}}^{\text{ES}} \tag{33}$$

$$C_{\text{de}}=\sum_{t=1}^{T}c_{\text{de}}(P_t^{\text{ES,cha}}+P_t^{\text{ES,dis}})\tau \tag{34}$$

$$C_{\text{EV}}=\sum_{t=1}^{T}[c_{\text{P}}P_t^{\text{EV,dis}}\tau+c_{\text{X}}(\bar{X}_t^{\text{EV}}-X_t^{\text{EV}})-c_{\text{buy}}^{\text{grid}}(P_t^{\text{EV,cha}}-P_t^{\text{EV,dis}})\tau] \tag{35}$$

$$C_{\text{HVAC}}=\sum_{t=1}^{T}c_{\text{H}}(P_t^{\text{HVAC,cha}}+P_t^{\text{HVAC,dis}})\tau \tag{36}$$

$$R_{\text{gird}}=\sum_{t=1}^{T}(c_{\text{sell}}^{\text{grid}}P_{\text{sell},t}^{\text{grid}}-c_{\text{buy}}^{\text{grid}}P_{\text{buy},t}^{\text{grid}})\tau \tag{37}$$

$$R_{\text{sv}}=\sum_{k=1}^{K}\sum_{t=1}^{T}c_{\text{sv}}(P_{k,t}^{\text{use,cha}}+P_{k,t}^{\text{use,dis}})\tau \tag{38}$$

$$R_{\text{tr}}=\sum_{k=1}^{K}\sum_{t=1}^{T}(c_{\text{sell}}^{\text{use}}P_{k,t}^{\text{use,dis}}-c_{\text{buy}}^{\text{use}}P_{k,t}^{\text{use,cha}})\tau \tag{39}$$

where r is the discount rate; Y is the planning horizon; c_{in}^{X} and c_{in}^{P} are the investment costs per unit capacity and per unit power of the PES, respectively; $\bar{X}_{\text{in}}^{\text{ES}}$ and $\bar{P}_{\text{in}}^{\text{ES}}$ are the upper capacity and power limits of the energy storage, respectively; K is the number of users that trade with the SES station; c_{ma} is the maintenance cost per unit of power for the PES; c_{de} is the loss cost factor of charging and discharging power of the PES; $P_t^{\text{ES,cha}}$ and $P_t^{\text{ES,dis}}$ are the charging and discharging power of the PES, respectively; c_{P} and c_{X} are the compensation factors of battery loss and user capacity satisfaction for EVs, respectively; $P_t^{\text{EV,cha}}$ and $P_t^{\text{EV,dis}}$ are the charging and discharging power of EVs, respectively; $P_t^{\text{HVAC,cha}}$ and $P_t^{\text{HVAC,dis}}$ are the charging and discharging power of HVAC clusters, respectively; c_{H} is the compensation factor of user satisfaction for HVAC clusters; $c_{\text{buy}}^{\text{grid}}$ and $c_{\text{sell}}^{\text{grid}}$ are the purchase and sale prices of electricity for the SES station transacting with the grid, respectively; $P_{\text{buy},t}^{\text{grid}}$ and $P_{\text{sell},t}^{\text{grid}}$ are the electricity purchased from and sold to the grid by the SES station, respectively; $c_{\text{buy}}^{\text{use}}$ and $c_{\text{sell}}^{\text{use}}$ are the charging and discharging transaction prices between the SES station and the user, respectively; c_{sv} is the energy storage service cost factor that the user needs to pay for charging and discharging; and $P_{k,t}^{\text{use,cha}}$ and $P_{k,t}^{\text{use,dis}}$ are the charging and discharging power that the SES station trades with user k, respectively.

B. Constraints

1) Capacity and Power Constraints of PES

The capacity and power of the PES need to satisfy a certain ratio. Equation (40) specifies the energy ratio constraint of the PES. Equation (41) is the power constraint of the PES.

$$\bar{X}_{\text{in}}^{\text{ES}}=\lambda\bar{P}_{\text{in}}^{\text{ES}} \tag{40}$$

$$0\le\bar{P}_{\text{in}}^{\text{ES}}\le P_{\text{in}}^{\max} \tag{41}$$

where λ is the energy ratio of the PES; and $P_{\text{in}}^{\max}$ is the upper power limit of the PES.

2) Operational Constraints of SES Station

Equations (42)-(47) represent the charging and discharging power constraints and energy constraints of the PES.

$$X_{t+1}^{\text{ES}}=\alpha^{\text{ES}}X_t^{\text{ES}}+\eta^{\text{ES,cha}}P_t^{\text{ES,cha}}+P_t^{\text{ES,dis}}/\eta^{\text{ES,dis}} \tag{42}$$

$$\underline{X}_{\text{in}}^{\text{ES}}\le X_t^{\text{ES}}\le\bar{X}_{\text{in}}^{\text{ES}} \tag{43}$$

$$P_t^{\text{ES}}=P_t^{\text{ES,cha}}-P_t^{\text{ES,dis}} \tag{44}$$

$$u_t^{\text{cha}}+u_t^{\text{dis}}\le 1 \tag{45}$$

$$0\le P_t^{\text{ES,cha}}\le u_t^{\text{cha}}\bar{P}_{\text{in}}^{\text{ES}} \tag{46}$$

$$0\le P_t^{\text{ES,dis}}\le u_t^{\text{dis}}\bar{P}_{\text{in}}^{\text{ES}} \tag{47}$$

where P_t^{ES} and X_t^{ES} are the charging and discharging power and capacity of the energy storage, respectively; $\underline{X}_{\text{in}}^{\text{ES}}$ is the lower capacity limit of the energy storage; $\eta^{\text{ES,cha}}$ and $\eta^{\text{ES,dis}}$ are the charging and discharging efficiencies of the energy storage, respectively; α^{ES} is the self-discharging rate; and u_t^{cha} and u_t^{dis} are the charging and discharging state variables of the energy storage, respectively, with $u_t^{\text{cha}}=1$ indicating charging and $u_t^{\text{dis}}=1$ indicating discharging.

Since (46) and (47) contain products of continuous and binary variables, these nonlinear terms can now be decoupled and linearized, resulting in the following formulations:

$$\begin{cases}0\le P_t^{\text{ES,cha}}\le u_t^{\text{cha}}P_{\text{in}}^{\max}\\ 0\le P_t^{\text{ES,dis}}\le u_t^{\text{dis}}P_{\text{in}}^{\max}\\ P_t^{\text{ES,cha}}\le\bar{P}_{\text{in}}^{\text{ES}}\\ P_t^{\text{ES,dis}}\le\bar{P}_{\text{in}}^{\text{ES}}\end{cases} \tag{48}$$

Furthermore, the SES station must comply with the GES constraints. Specifically, the operation of the EV clusters needs to satisfy the flexible operation region of the GES capacity shown in (15)-(17). Similarly, the operation of the HVAC clusters needs to satisfy the flexible operation region of the GES capacity shown in (18)-(20).

The SES station should meet the base load demand of the distributed resources, the power demand traded with the grid, and the power demand traded with the users, as shown in (49).

$$P_t^{\text{ES,dis}}-P_t^{\text{ES,cha}}+P_t^{\text{EV}}+P_t^{\text{HVAC}}=P_{\text{base},t}^{\text{HVAC}}-P_{\text{buy},t}^{\text{grid}}+P_{\text{sell},t}^{\text{grid}}+\sum_k(P_{k,t}^{\text{use,dis}}-P_{k,t}^{\text{use,cha}}) \tag{49}$$

At the same time, the SES station also needs to satisfy the power balance constraint for PES, as shown in (50).

$$\sum_{t=1}^{T}(P_t^{\text{ES,dis}}-P_t^{\text{ES,cha}})=0 \tag{50}$$

V. DRO Model Solving Algorithm

The DRO model can be solved using the column-and-constraint generation (C&CG) algorithm, which decomposes it into a master problem (MP) and a sub-problem (SP), effectively reducing the problem complexity. During the solution process, new variables and constraints generated by the SP are iteratively introduced into the MP. This iterative process causes the lower bound L_B of the objective from the MP and the upper bound U_B of the objective from the SP to converge, ultimately yielding the global optimal solution.

A. MP

The MP of the DRO model aims to find the optimal configuration capacity of the PES and the optimal scheduling strategy of the SES station, given the known probability distribution values of scenarios. Its mathematical model is given as:

$$\min_{\boldsymbol{x}} \left(F_{\text{in}}(\boldsymbol{x})+\theta\right) \tag{51}$$

s.t.

$$h(\boldsymbol{x})\leq 0 \tag{52}$$

$$\theta\geq \sum_{j=1}^{J} p_j^{(l)} r(\boldsymbol{x},\xi_j,\boldsymbol{y}_j^{(l)}) \tag{53}$$

$$g(\boldsymbol{x},\xi_j,\boldsymbol{y}_j^{(l)})\leq 0 \tag{54}$$

where θ is the SP slack variable; $h(\cdot)$ denotes the constraints that are dependent solely on the first-stage decisions; $p_j^{(l)}$ is the probability distribution value of scenario j in the l^{th} iteration, which is a known quantity returned by the SP; $\boldsymbol{x}$ is the first-stage variable, which denotes the configuration capacity and power of the PES; ξ_j is the ambiguous variable of scenario j; $\boldsymbol{y}_j^{(l)}$ is the second-stage variable of scenario j in the l^{th} iteration introduced for the MP, which denotes the power of the SES station trading with the grid and the simulated operating power of each unit; $r(\cdot)$ is the objective function of the inner minimum problem; and $g(\cdot)$ denotes the constraints related to the second-stage operation.

Equation (52) denotes the constraints related only to the first-stage energy storage configuration, including (40) and (41). Equation (53) denotes the introduced auxiliary variable constraints. Equation (54) denotes the constraints related to the second-stage operation, as given by (15)-(20), (42)-(45), and (48)-(50).

B. SP

The SP of the DRO model aims to identify the worst-case probability distribution based on the optimal operational results of scenarios, given a fixed energy storage configuration. Its mathematical model can be expressed as:

$$\max_{p_j\in\Omega}\left(\sum_{j=1}^{J} p_j \min_{\boldsymbol{y}_j\in U(\boldsymbol{x},\xi_j)} F_{\text{op}}(\boldsymbol{x}^*,\xi_j,\boldsymbol{y}_j)\right) \tag{55}$$

s.t.

$$g(\boldsymbol{x}^*,\xi_j,\boldsymbol{y}_j)\leq 0 \tag{56}$$

where $\boldsymbol{x}^*$ is the first-stage configuration result, which is a known parameter; and $U(\boldsymbol{x},\xi_j)$ is the feasible operation region for $\boldsymbol{y}_j$, given the first-stage variables and the ambiguous variables.

The constraint (56) pertains to the operational constraints related to trading, including constraints (15)-(20), (42)-(45), and (48)-(50).

The mathematical model of the SP is a max-min problem. Since the scheduling problem of the SES station in each scenario is independent, a parallel solving method can be employed. Therefore, the SP can be transformed into the following two optimization problems for sequential solution.

The objective function of the scheduling problem of the SES station is given by (57), and the constraints are defined by (56).

$$r(\boldsymbol{x}^*,\xi_j)=\min_{\boldsymbol{y}_j\in U(\boldsymbol{x},\xi_j)} F_{\text{op}}(\boldsymbol{x}^*,\xi_j,\boldsymbol{y}_j) \tag{57}$$

where $r(\cdot)$ is the objective function value of the SP for each uncertain scenario.

The objective function for the optimization problem of identifying the worst-case probability distribution of scenarios is expressed by (58), and the ambiguous variable set of probability distributions in the flexible operation region of GES capacity is described by (29).

$$\max_{p_j\in\Omega}\sum_{j=1}^{J} p_j r(\boldsymbol{x},\xi_j) \tag{58}$$

By solving the two optimization problems (57) and (58) alternately, the worst-case probability distribution of scenarios can be obtained and subsequently transmitted to the MP for the next iteration. The flowchart of the DRO model solving algorithm is shown in Fig. 3.

VI. Case Study

Three different types of prosumers within a park are selected as research subjects. Each prosumer is directly connected to the SES station, where the ratio of the maximum power to the capacity for the configured energy storage is set to be 2.74. The EV is modeled using parameters of the Tesla Model Y. The K-means clustering algorithm is applied to the sampled data of EV and HVAC clusters, reducing the number of scenarios to four typical ones. The implementation is performed in MATLAB 2017b, and the problem is solved using the commercial solver Gurobi-11.0. The basic simulation parameters are presented in Table I.

In this paper, the following four different cases are designed to test the validity of the SES station and the proposed GES models for EV and HVAC clusters.

Case 1: prosumers configure energy storage individually, and EVs and HVAC systems participate in the market with ordered charging mode and traditional air conditioning mode, respectively.

Case 2: with SES station, EV and HVAC clusters participate in the market with ordered charging mode and traditional air conditioning mode, respectively.

Case 3: without SES station, EV and HVAC clusters participate in the market with their GES models under operator scheduling.

Case 4: with SES station, EV and HVAC clusters participate in the market with their GES models under operator scheduling.

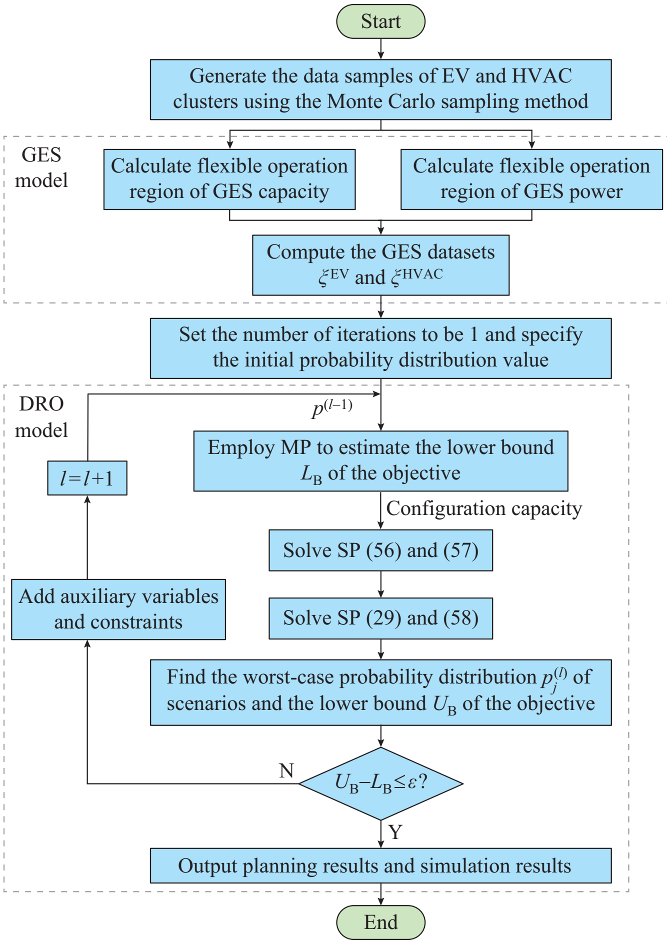

Fig. 3. Flowchart of DRO model solving algorithm.

TABLE I
BASIC SIMULATION PARAMETERS

Parameter	Value
Initial SOC of PES	0.4
Investment cost per unit power (CNY/kW)	1897
Discharging efficiency of battery	0.95
Degradation coefficient of PES (CNY/kW)	0.5
Coefficient of the maximum power and capacity of PES	2.74
Upper power limit of EVs (kW)	6.5
Battery capacity of EVs (kWh)	60
Lower SOC limit of EVs	0.1
Time-of-use rate (CNY/kWh)	[1.4, 0.8, 0.55]
Thermal resistance range (°C/kW)	[2, 3]
Upper power limit of HVAC systems (kW)	3
Investment cost per unit capacity (CNY/kW)	1200
Charging efficiency of battery	0.95
Average daily maintenance coefficient of PES (CNY/kW)	0.08
Service life of PES (year)	10
Charging/discharging efficiency range of EVs	[0.85, 0.95]
Lower power limit of EVs (kW)	–6.5
Upper SOC limit of EVs	0.9
Number of EVs	200
Thermal capacity range (kWh/°C)	[2, 3]
Number of HVAC systems	2000
Temperature setting range (°C)	[20, 24]

TABLE II
PLANNING RESULTS OF SES STATIONS UNDER DIFFERENT CASES

Case	Energy storage capacity (kWh)	Investment cost (CNY)	Total revenue (CNY)	Daily equivalent cycle count
Case 1	3295.60	3141.89		1.6869
Case 2	2408.98	2296.63	1761.59	1.8958
Case 3			2072.30	
Case 4	1384.57	1320.00	2820.48	1.9479

A. Analysis of Different Configurations of SES Station

Table II presents the planning results of SES stations under different cases. As can be observed, Case 1 corresponds to individual energy storage configurations for prosumers, with a total capacity of 3295.60 kWh. However, the utilization rate of these individual energy storage resources remains low. In contrast, Case 2, through the implementation of an SES station, leverages the load diversity and renewable energy output complementarity among different prosumers, thereby significantly reducing the underutilization of energy storage resources. The energy storage capacity in Case 2 is 26.90% lower than that in Case 1. Case 3 further incorporates the energy storage characteristics of proposed GES models for EV and HVAC clusters, enhancing the resource utilization and increasing the total revenue through peak shaving and valley filling. While still employing an SES station, Case 4 leverages the flexible regulation capabilities of demand-side resources to enable more effective peak shaving and valley filling. It saves 1001.27 kWh of energy storage capacity compared with Case 2, which is a 42.52% reduction in configuration capacity. The daily equivalent cycle count is the ratio of the average daily charging or discharging capacity to the actual energy storage capacity. The daily equivalent cycle count of the PES increases from 1.6869 in Case 1 to 1.9479 in Case 4.

The coordination of GES within the SES station enables the SES operator to achieve a substantial reduction in investment and operating costs of PES, concurrently increasing the flexibility of the controllable resources. This significantly enhances the profitability of the SES operator, yielding profit increases of 26.53% over Case 3 and 37.54% over Case 2. Following the integration of GES into the operation of SES station, the static investment payback period of PES is reduced from 8.75 years to 3.14 years, and the return on investment increases by 20.42%. The typical daily operating curves of HVAC and EV clusters are shown in Appendix A Fig. A1 and Fig. A2, respectively.

Figure 4 presents the power optimization results for the first typical scenario of the SES station in Case 4. Although the GES models for EV and HVAC clusters discharge less frequently than the PES, their discharging capacity is considerable. The GES plays a substantial role in the operation of the SES station, by effectively reducing its required configuration capacity and providing prosumers with more flexible and adjustable resources. Furthermore, although the SES operator purchases substantial electricity from the grid, this cost is not borne by the operator, as it is primarily used to meet EV charging demand.

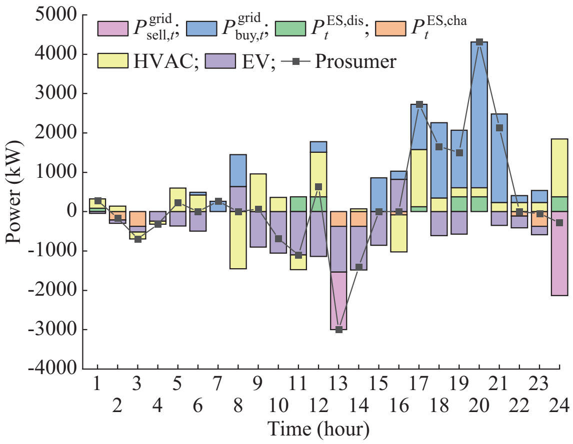

Fig. 4. Power optimization results for first typical scenario of SES station in Case 4.

B. Accuracy Analysis of Proposed GES Model for EV Clusters

This subsection evaluates the proposed GES model for EV clusters against the traditional model (TM) and the VB model [21] to ascertain its accuracy. The power and capacity scheduling results of different models are shown in Fig. 5 and Fig. 6, respectively. EV clusters are sampled using the Monte Carlo method, with charging and discharging efficiencies assumed to follow a uniform distribution $\eta_i^{\text{cha}} \sim U[0.85, 0.95]$ and $\eta_i^{\text{dis}} \sim U[0.85, 0.95]$.

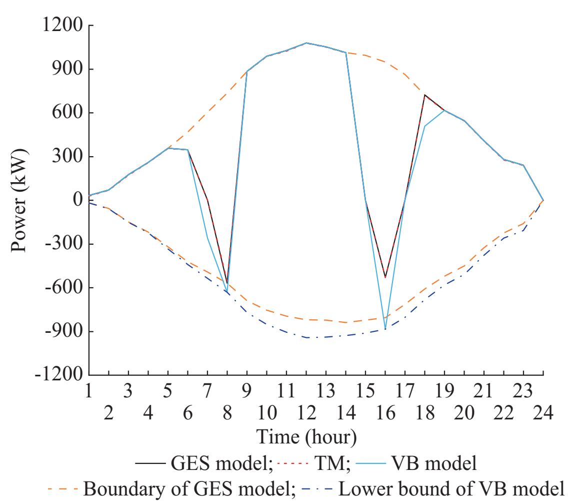

Fig. 5. Power scheduling results of different models.

A critical criterion for an aggregation model is the accuracy of its replication of the external characteristics of clusters. In this study, the capacity of the proposed GES model for EV clusters is compared with the ideal battery capacity of the TM (denoted as ideal capacity), while the capacity of the VB model is compared with the real battery capacity of the TM (denoted as real capacity), as shown in Fig. 6.

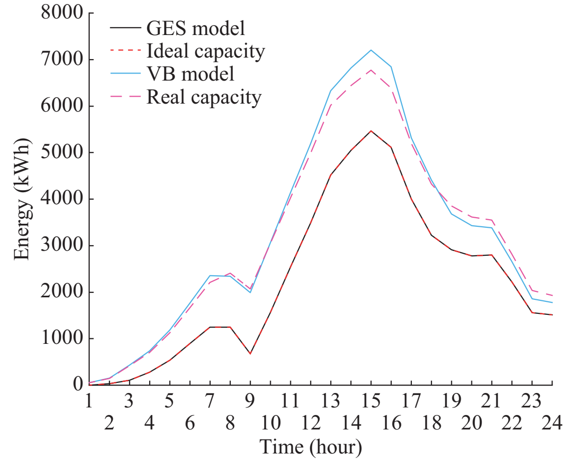

Fig. 6. Capacity scheduling results of different models.

As shown in Fig. 5, the power calculated by the proposed GES model for EV clusters closely aligns with that for the EV cluster by the TM. The SES operator reduces operating costs by curtailing EV charging power during the periods of the 6th-9th hours and 14th-18th hours and strategically discharging some EVs. In contrast, the VB model yields lower operating power than the TM, as it does not consider the charging and discharging efficiencies. Since the VB model neglects the discharging efficiencies when defining the lower boundary of the flexible operation region of the GES power, its lower boundary falls below that of the flexible operation region of GES power. Therefore, the dispatch power determined by the VB model remains below the flexible operation region of the actual power at the 8th hour and the 16th hour. It can also be observed from Fig. 6 that the capacity of the proposed GES model aligns with the ideal capacity, while a gap exists between the capacity of the VB model and the actual capacity. This discrepancy is particularly evident during the aforementioned discharging periods of EV clusters. Although the aggregated capacity of the proposed GES model does not equal the sum of capacities of all individual EVs, its key strength lies in satisfying the operational power constraints within the feasible operation region. This ensures a precise capture of the external power characteristics at the aggregate level.

A detailed comparison of the planning results of SES stations under the VB model and the proposed GES model for EV clusters is conducted using the parameters in the first typical scenario, which is shown in Table III. The results indicate that while the energy storage capacity configured by the proposed GES model for EV clusters is higher than that by the VB model, the proposed GES model for EV clusters yields higher total revenue. This discrepancy occurs because the VB model neglects the charging and discharging efficiencies of EV clusters, leading to an overestimated feasible operation region. In contrast, the proposed GES model for EV clusters accounts for the charging and discharging efficiencies of EV clusters, which makes the scheduling results better aligned with the actual behavior of EV clusters and thus more reliable. Due to neglecting the charging and discharging efficiencies, the VB model must purchase additional electricity from the grid during operation to compensate for the energy shortfall during the discharging periods of EV clusters, resulting in a daily loss of 720.5944 CNY. Conversely, the proposed GES model for EV clusters, which is more accurate and conservative, anticipates an energy surplus during the periods of the 6^{th}-8^{th} hours and 15^{th}-19^{th} hours, which can be sold back to the grid, yielding a profit of 35.7131 CNY. These results demonstrate that the proposed GES model for EV clusters more accurately captures both the flexible operation region and external characteristics of EV clusters.

TABLE III
COMPARISON OF PLANNING RESULTS OF SES STATIONS UNDER DIFFERENT MODELS

Model	Energy storage capacity (kWh)	Investment cost (CNY)	Operating revenue (CNY)	Compensation cost (CNY)	Total revenue (CNY)
VB	1616.10	1540.72	5254.22	720.59	2992.89
GES	1888.89	1800.80	5410.34	–35.71	3573.82

C. Comparative Analysis of Different Methods

1) Comparison with Deterministic Capacity Configuration Method

The proposed method is compared with the deterministic capacity configuration method. The planning results of SES stations are simulated in the worst-case scenario to assess the risk control ability of the two methods, and the comparison is shown in Table IV. As shown in Table IV, employing the deterministic capacity configuration method to configure PES can achieve more abundant capacity configuration and higher operating revenue. Due to the significant influence of user behavior, the GES parameters calculated using the deterministic capacity configuration method exhibit considerable fluctuations. This results in overcapacity and high investment costs, which could entail risk loss cost in extreme scenarios of up to 237.82 CNY. In contrast, the proposed method reduces the risk loss cost in extreme scenarios to only 27.69 CNY, demonstrating superior risk management capability.

TABLE IV
COMPARISON OF PLANNING RESULTS OF SES STATIONS UNDER DIFFERENT METHODS

Method	Energy storage capacity (kWh)	Investment cost (CNY)	Operating revenue (CNY)	Risk loss cost (CNY)	Total revenue (CNY)
Deterministic	1779.18	1696.20	4701.99	237.82	2767.97
Proposed	1384.57	1320.00	4140.48	27.69	2792.78

2) Comparison with Other Models

The proposed DRO model is compared with the SO and RO models. EV clusters and HVAC clusters with varying sample sizes are selected to illustrate the advantages of the proposed DRO model, and the results are presented in Fig. 7.

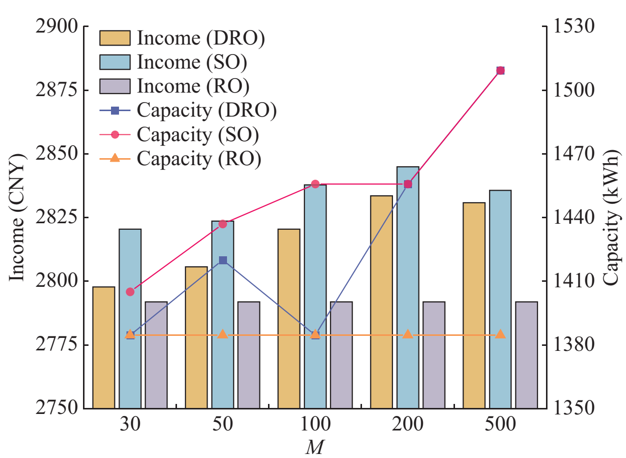

Fig. 7. Comparison of results of different models.

As shown in Fig. 7, the proposed DRO model enables flexible adjustment of conservativeness through sample size variation. This allows for managing uncertain risks while considering economic efficiency. When the sample size reaches 200, the results converge to those of the SO model. For comparison, using the traditional RO model instead of the proposed DRO model results in an operating profit of 2791.89 CNY. This overly conservative model leads to reduced operating profit. The results show that the proposed DRO model strikes a balance between the economic efficiency of the SO model and the conservatism of the RO model, and provides tunable levels of economy and robustness.

D. Sensitivity Analysis on Uncertainty of EVs and HVAC Systems

Different prediction error multipliers are used to perform sensitivity analysis [29] on the uncertainty of EVs and HVAC systems, and the results are shown in Fig. 8. As the multiplier increases, the SES operator fails to provide sufficient discharging capacity, compelling the operator to purchase electricity at elevated grid prices to fulfil contracts and thereby progressively escalating compensation costs. Since EVs have more ambiguous variables and higher volatility than HVAC systems, the compensation costs associated with EVs demonstrate more pronounced changes as the multiplier increases.

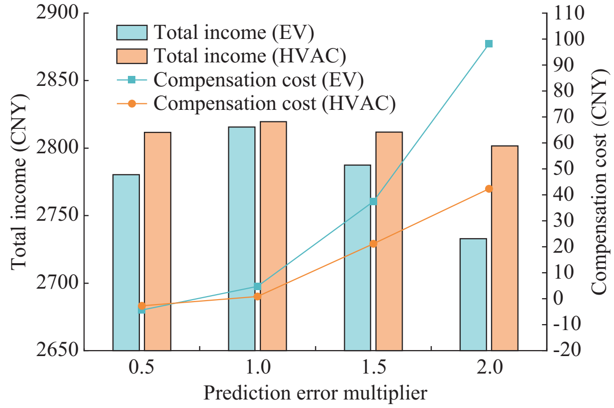

Fig. 8. Sensitivity analysis results on uncertainty of EVs and HVAC systems.

VII. Conclusion

To harness the flexible scheduling potential of numerous and heterogeneous distributed resources while mitigating associated uncertainties, we employ a two-stage distributionally robust capacity configuration method for SES that accounts for the flexibility and uncertainty of distributed resources. Combined with simulation analysis, the following conclusions are drawn.

1) The proposed shared system architecture for the GES, which integrates virtual energy storage like EVs and HVAC systems with the PES, can reduce the investment and operation costs of the PES while increasing operating revenue.

2) The proposed GES model for EV clusters provides a more accurate aggregation model of their flexible operation region and external characteristics compared with existing aggregation models.

3) To address uncertainties of demand-side EVs and HVAC systems, the proposed DRO model can effectively balance the benefits of SO and RO models. The proposed DRO model strikes a balance between economic efficiency and robustness in the capacity configuration problem of SES.

Future work will further investigate the optimal site selection method for SES station. Additionally, the interaction characteristics between prosumers and GES models such as EVs and HVAC systems will also be a key focus of future research.

Appendix A

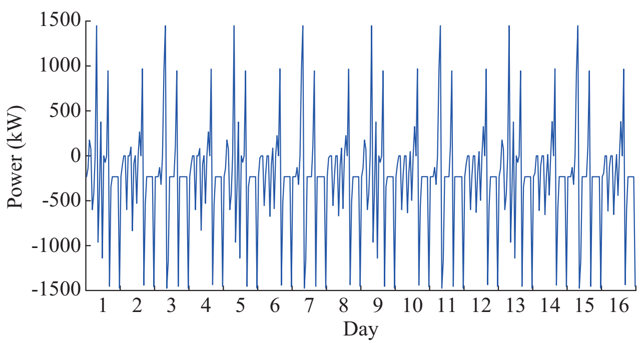

Fig. A1. Typical daily operating curve of HVAC clusters.

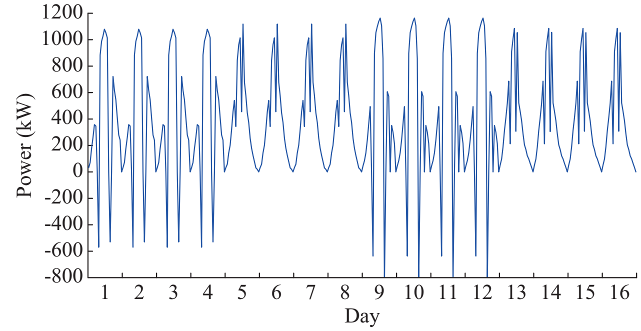

Fig. A2. Typical daily operating curve of EV clusters.

References

[1] J. Gao, F. Gao, Y. Yang *et al.*, "Configuration optimization and benefit allocation model of multi-park integrated energy systems considering electric vehicle charging station to assist services of shared energy storage power station," *Journal of Cleaner Production*, vol. 336, p. 130381, Feb. 2022.

[2] Y. Qiu, Q. Li, S. Li *et al.*, "Lifecycle collaborative planning for traction power supply systems with integrated energy access," *IEEE Transactions on Transportation Electrification*, vol. 11, no. 1, pp. 5055-5068, Feb. 2025.

[3] R. Dai, R. Esmaeilbeigi, and H. Charkhgard, "The utilization of shared energy storage in energy systems: a comprehensive review," *IEEE Transactions on Smart Grid*, vol. 12, no. 4, pp. 3163-3174, Jul. 2021.

[4] L. Yao, B. Yang, H. Cui *et al.*, "Challenges and progresses of energy storage technology and its application in power systems," *Journal of Modern Power Systems and Clean Energy*, vol. 4, no. 4, pp. 519-528, Oct. 2016.

[5] J. Xiao, Y. Yang, S. Cui *et al.*, "A new energy storage sharing framework with regard to both storage capacity and power capacity," *Applied Energy*, vol. 307, p. 118171, Feb. 2022.

[6] Y. Zhuang, Z. Li, Q. Tan *et al.*, "Multi-time-scale resource allocation based on long-term contracts and real-time rental business models for shared energy storage systems," *Journal of Modern Power Systems and Clean Energy*, vol. 12, no. 2, pp. 454-465, Mar. 2024.

[7] W. Tong, Z. Lu, Y. Chen *et al.*, "Enhancing modular gravity energy storage plants: a hybrid strategy for optimal unit capacity configuration," *Applied Energy*, vol. 378, p. 124774, Jan. 2025.

[8] S. Lai, J. Qiu, and Y. Tao, "Credit-based pricing and planning strategies for hydrogen and electricity energy storage sharing," *IEEE Transactions on Sustainable Energy*, vol. 13, no. 1, pp. 67-80, Jan. 2022.

[9] J. Li, Z. Fang, Q. Wang *et al.*, "Optimal operation with dynamic partitioning strategy for centralized shared energy storage station with integration of large-scale renewable energy," *Journal of Modern Power Systems and Clean Energy*, vol. 12, no. 2, pp. 359-370, Mar. 2024.

[10] Q. Wang, X. Zhang, C. Yi *et al.*, "A novel shared energy storage planning method considering the correlation of renewable uncertainties on the supply side," *IEEE Transactions on Sustainable Energy*, vol. 13, no. 4, pp. 2051-2063, Oct. 2022.

[11] J. Han, Y. Fang, Y. Li *et al.*, "Optimal planning of multi-microgrid system with shared energy storage based on capacity leasing and energy sharing," *IEEE Transactions on Smart Grid*, vol. 16, no. 1, pp. 16-31, Jan. 2025.

[12] T. Zhang, C. Chen, L. Ma *et al.*, "Multi-step clustering and generalized Nash bargaining-based planning strategy of community-shared energy storage for large-scale prosumers," *IEEE Transactions on Sustainable Energy*, vol. 15, no. 2, pp. 1013-1027, Apr. 2024.

[13] P. Du, B. Huang, Z. Liu *et al.*, "Real-time energy management for net-zero power systems based on shared energy storage," *Journal of Modern Power Systems and Clean Energy*, vol. 12, no. 2, pp. 371-380, Mar. 2024.

[14] Y. Pu, Q. Li, S. Huo *et al.*, "Optimal configuration for shared electric-hydrogen energy storage for multiple integrated energy systems with mobile hydrogen transportation," *Renewable Energy*, vol. 237, p. 121828, Dec. 2024.

[15] F. D'Ettorre, M. Banaei, R. Ebrahimy *et al.*, "Exploiting demand-side flexibility: state-of-the-art, open issues and social perspective," *Renewable and Sustainable Energy Reviews*, vol. 165, p. 112605, Sept. 2022.

[16] S. Barot and J. A. Taylor, "A concise, approximate representation of a

collection of loads described by polytopes," *International Journal of Electrical Power & Energy Systems*, vol. 84, pp. 55-63, Jan. 2017.

[17] X. Zhao, L. Li, Y. Tao *et al*., "Aggregated operation of heterogeneous small-capacity distributed energy resources in peer-to-peer energy trading," *International Journal of Electrical Power & Energy Systems*, vol. 141, p. 108162, Oct. 2022.

[18] X. Wang, H. Jia, Z. Wang *et al*., "A real time peer-to-peer energy trading for prosumers utilizing time-varying building virtual energy storage," *International Journal of Electrical Power & Energy Systems*, vol. 155, p. 109547, Jan. 2024.

[19] S. He, H. Gao, Z. Tang *et al*., "Worst CVaR based energy management for generalized energy storage enabled building-integrated energy systems," *Renewable Energy*, vol. 203, pp. 255-266, Feb. 2023.

[20] H. Hao, D. Wu, J. Lian *et al*., "Optimal coordination of building loads and energy storage for power grid and end user services," *IEEE Transactions on Smart Grid*, vol. 9, no. 5, pp. 4335-4345, Sept. 2018.

[21] J. Li, Q. Ai, S. Yin *et al*., "An aggregator-oriented hierarchical market mechanism for multi-type ancillary service provision based on the two-loop Stackelberg game," *Applied Energy*, vol. 323, p. 119644, Oct. 2022.

[22] Q. Li, F. Dong, G. Zhou *et al*., "Co-optimization of virtual power plants and distribution grids: emphasizing flexible resource aggregation and battery capacity degradation," *Applied Energy*, vol. 377, p. 124519, Jan. 2025.

[23] J. Zhu, Q. Ai, and J. Li, "Capacity allocation method for generalized shared energy storage based on distributionally robust optimization," *Automation of Electric Power Systems*, vol. 48, No. 8, pp. 185-194, Apr. 2024.

[24] J. L. Mathieu, M. G. Vaya, and G. Andersson, "Uncertainty in the flexibility of aggregations of demand response resources," in *Proceedings of 39th Annual Conference of the IEEE Industrial Electronics Society*, Vienna, Austria, Nov. 2013, pp. 1-6.

[25] Y. Chen, X. Li, and Z. Zhang, "Risk assessment of rail transit systems with variable renewable energy based on uncertain random theory," *International Journal of Electrical Power & Energy Systems*, vol. 164, p. 110441, Mar. 2025.

[26] H. Pandžić, J. M. Morales, A. J. Conejo *et al*., "Offering model for a virtual power plant based on stochastic programming," *Applied Energy*, vol. 105, pp. 282-292, May 2013.

[27] Y. Chen, Z. Zhang, H. Chen *et al*., "Robust UC model based on multi-band uncertainty set considering the temporal correlation of wind/load prediction errors," *IET Generation*, *Transmission & Distribution*, vol. 14, no. 2, pp. 180-190, Jan. 2020.

[28] Y. Li, M. Han, M. Shahidehpour *et al*., "Data-driven distributionally robust scheduling of community integrated energy systems with uncertain renewable generations considering integrated demand response," *Applied Energy*, vol. 335, p. 120749, Apr. 2023.

[29] Z. Liu, Y. Chen, Z. Zhang *et al*., "Identification of vulnerable nodes and sensitivity analysis of control parameters for multiple grid-connected converter systems," *IEEE Transactions on Sustainable Energy*, vol. 16, no. 3, pp. 1602-1612, Jul. 2025.

Ning Zhang received the bachelor's degree in electrical engineering from North China Electric Power University, Beijing, China, in 2022, and has been pursuing the doctor's degree in electrical engineering from the same university since 2022. Her research interests include optimal scheduling of integrated energy system, power system planning, and planning and operation of zero-carbon park.

Yanbo Chen received the B.S. degree in electrical engineering from Huazhong University of Science and Technology, Wuhan, China, in 2007, the M.S. degree in electrical engineering from China Electric Power Research Institute, Beijing, China, in 2010, and the Ph.D. degree in electrical engineering from Tsinghua University, Beijing, China, in 2013. He is currently a Professor with North China Electric Power University, Beijing, China, and an Outstanding Young Energy Scientist of China Energy Research Society. He is also a Senior Member of IEEE, CIGRE Member, editorial board member of Journal of Modern Power Systems and Clean Energy, and associate editor or editorial board member of several journals. His research interests include planning and operation of power system.

Zhi Zhang received the B.S. degree in electrical engineering from China Three Gorges University, Yichang, China, in 2017, and the M.S. and Ph.D. degrees in electrical engineering from North China Electric Power University, Beijing, China, in 2020 and 2023, respectively. Since 2023, he has been with the School of Electrical and Electronic Engineering, North China Electric Power University, where he is currently an Associate Professor. His main research interests include operation and control of power system.

Haoxin Tian received the B.S. and M.S. degrees in electrical engineering from North China Electric Power University, Baoding, China, in 2018 and 2021, respectively. He is currently pursuing the Ph.D. degree in electrical engineering at North China Electric Power University, Beijing, China. His research interests include planning and operation of power system with renewable energy.